arXiv:astro-ph/9609113v1 17 Sep 1996

The SBF Survey of Galaxy Distances. I.

Sample Selection, Photometric Calibration, and the Hubble Constant[1]

John L. Tonry[2] and John P. Blakeslee[2]
Physics Dept. Room 6-204, MIT, Cambridge, MA 02139;

Edward A. Ajhar[2]
Kitt Peak National Observatory, National Optical Astronomy Observatories, P.O. Box 26732
Tucson, AZ 85726;

Alan Dressler
Carnegie Observatories, 813 Santa Barbara St., Pasadena, CA 91101

ABSTRACT

We describe a program of surface brightness fluctuation (SBF) measurements for determining galaxy distances. This paper presents the photometric calibration of our sample and of SBF in general. Basing our zero point on observations of Cepheid variable stars we find that the absolute SBF magnitude in the Kron-Cousins I band correlates well with the mean $(V-I)_0$ color of a galaxy according to

$$\overline{M}_I = (-1.74 \pm 0.07) \; + \; (4.5 \pm 0.25)\,[(V-I)_0 - 1.15]$$

for $1.0 < (V-I) < 1.3$. This agrees well with theoretical estimates from stellar population models.

Comparisons between SBF distances and a variety of other estimators, including Cepheid variable stars, the Planetary Nebula Luminosity Function (PNLF), Tully-Fisher (TF), D_n–σ, SNII, and SNIa, demonstrate that the calibration of SBF is universally valid and that SBF error estimates are accurate. The zero point given by Cepheids, PNLF, TF (both calibrated using Cepheids), and SNII is in units of Mpc; the zero point given by TF (referenced to a distant frame), D_n–σ, and SNIa is in terms of a Hubble expansion velocity expressed in km/s. Tying together these two zero points yields a Hubble constant of

$$H_0 = 81 \pm 6 \text{ km/s/Mpc.}$$

As part of this analysis, we present SBF distances to 12 nearby groups of galaxies where Cepheids, SNII, and SNIa have been observed.

---

[1]Observations in part from the Michigan-Dartmouth-MIT (MDM) Observatory.

[2]Guest observers at the Cerro Tololo Interamerican Observatory and the Kitt Peak National Observatory, National Optical Astronomy Observatories, which are operated by AURA, Inc., under cooperative agreement with the National Science Foundation.

Subject headings: galaxies: distances and redshifts — galaxies: clusters: individual – cosmology: distance scale

1. Introduction and Sample Selection

1.1. Background

The surface brightness fluctuation (SBF) method of distance determination works by measuring the ratio of the second and first moments of the stellar luminosity function in a galaxy. This ratio, called $\overline{L}$, is then the luminosity-weighted, average luminosity of a stellar population and is roughly equal to the luminosity of a single giant star. In terms of magnitudes, this quantity is represented as $\overline{M}$, the absolute "fluctuation magnitude." What we measure, of course, is the apparent fluctuation magnitude in a particular photometric band, in our case the I band, $\overline{m}_I$. In order to be useful as a distance estimator, $\overline{m}_I$ must be calibrated, either empirically, by tying the measurements to the Cepheid distance scale, or theoretically, according to stellar population synthesis models.

Tonry and Schneider (1988) were the first to quantify the SBF phenomenon. Their method was based on a measurement of the amount of power on the scale of the point spread function in the power spectrum of a CCD image. They applied this method to images of the galaxies M32 and NGC 3379. Subsequent work by Tonry, Luppino, and Schneider (1988) and Tonry, Ajhar, & Luppino (1989, 1990) revised and refined the analysis techniques and presented further observations in V, R, and I of early-type galaxies in Virgo, Leo, and the Local Group. Tonry et al. (1990) found that the I band was most suitable for measuring distances and attempted to calibrate the SBF method theoretically using the Revised Yale Isochrones (Green, Demarque, & King 1987). There were obvious problems with this calibration, however, so a completely empirical calibration for $\overline{M}_I$ was presented by Tonry (1991). The calibration was based on the variation of $\overline{m}_I$ with $(V-I)_0$ color in the Fornax cluster and took its zero point from the Cepheid distance to M31. Tonry used this calibration to derive the Hubble constant. A detailed review of the modern SBF technique can be found in Jacoby et al. (1992), which also provides some historical context for the method.

In recent years, the SBF technique has been used to measure distances and study a variety of stellar populations in several different bands. K-band SBF observations have been reported by Luppino & Tonry (1993), Pahre & Mould (1994), and Jensen, Luppino, & Tonry (1996). These studies find that $\overline{m}_K$ is also a very good distance estimator. Dressler (1993) has measured I-band SBF in Centaurus ellipticals, finding evidence in support of the Great Attractor model. Lorenz et al. (1993) have measured I-band SBF in Fornax, and Simard & Pritchet (1994) have reported distances to two Coma I galaxies using V-band SBF observations. Ajhar & Tonry (1994) reported measurements of $\overline{m}_I$ and $\overline{m}_V$ for 19 Milky Way globular clusters and considered the implications for both the distance scale and stellar populations. Tiede, Frogel, & Terndrup (1995) measured

$\overline{m}_I$ and $\overline{m}_V$ for the bulge of the Milky Way and derived the distance to the Galactic center. Sodemann & Thomsen (1995, 1996) have used fluctuation colors and radial gradients to investigate stellar populations in galaxies. Finally, an enormous amount of progress has been achieved on the theoretical SBF front through the stellar population models of Worthey (1993a,b, 1994), Buzzoni (1993, 1995), and Yi (1996).

1.2. Genesis of the SBF Survey

When it became apparent that I-band SBF observations could indeed provide accurate and reliable distances to galaxies, we undertook a large survey of nearby galaxies. The sample selection is not precisely defined because the measurement of SBF depends on a number of criteria which are not ordinarily cataloged, such as dust content. In addition, because the measurement of SBF is fairly expensive in terms of telescope time and quality of seeing, it simply was not possible to observe all early-type galaxies within some magnitude limit out to a redshift which is large enough to make peculiar velocities negligible. Nevertheless, we have tried to manage fairly complete coverage of early-type galaxies within 2000 km/s and brighter than $B = 13.5$, and we have significant coverage beyond those limits.

Comparison with the Third Reference Catalog of Bright Galaxies (de Vaucouleurs et al. 1991) reveals that of the early-type galaxies ($T < 0$) with $B \leq 13.5$ in the RC3, we have observed 76% with heliocentric velocity $v < 1000$ km/s, 73% with $1000 < v < 1400$, 64% with $1400 < v < 2000$, 49% with $2000 < v < 2800$, and we have data for more than 40 galaxies with $v > 2800$ km/s. Virtually all of the galaxies closer than $v < 2000$ where we lack data are S0s for which measuring SBF is complicated by dust and/or disk/bulge problems, and since many of them are in the cores of clusters such as Virgo, we do not regard their distances as being important enough to delay completion of our survey. The survey is, however, an ongoing project, with some data still to be reduced. About 50% of our sample is listed as E galaxies ($T \leq -4$), about 40% as S0s, and 10% as "spirals" ($T \geq 0$). Our sample of galaxies is drawn from the entire sky, and the completeness was mainly driven by the vicissitudes of weather and telescope time, so the sampling is fairly random. The survey includes a large number of galaxies in the vicinity of the Virgo supercluster, and the next paper in this series will present an analysis of their peculiar motions.

The following section describes the SBF survey in more detail, including the observations, photometric reductions, and consistency checks. In Section 3 we use our observations of galaxies in groups to derive the dependence of $\overline{M}_I$ on $(V-I)_0$. Seven of these groups also have Cepheid distances, which we use to set the zero point of the $\overline{M}_I$–$(V-I)$ relation. This new $\overline{M}_I$ calibration agrees well with theory and supersedes the old calibration of Tonry (1991). We then compare our distances to those found using a number of other methods. In Section 4 we discuss the tie to the large-scale Hubble flow and implications for the value of H_0. The final section provides a summary of our main conclusions.

2. Observations and Reductions

All in all, the SBF survey extends over some 40 observing runs at 6 telescopes. Table 1 lists these runs along with some salient information. Note that the date of the run is coded in the name as (Observatory)MMYY; the remaining columns are described below.

The normal observing procedure when the skies were clear was to obtain sky flats each night and observe a number of Landolt standard stars. We preferred observing the faint standard star fields of Landolt (1992) in which there are several stars per CCD field and where the observations are long enough that shutter timing is not a problem. Table 2 gives our usual fields. During a typical night we would observe about 10 fields comprising perhaps 50 stars over a range of airmasses from 1.1 to 2.0. We also strived to observe stars over a wide range of color ranging from $0 < (V-I) < 2$. Because there is substantial fringing seen in the I band with thin CCDs, at some point in a run we would spend several hours looking at a blank field in order to build up a "fringe frame". We have found the fringing pattern for a given CCD and filter (although not the amplitude) to be remarkably stable from night to night (even year to year). Hence, a single fringe frame was used to correct an entire run's data, and we usually collected a new one for each run.

The reductions of the photometry proceed by bias subtraction, flattening, and following Landolt (1992), summing the net flux from photometric standards within a $14''$ aperture. We also estimate a flux error from the sky brightness and variability over the image and remove any stars whose expected error is greater than 0.02 magnitude. Once all the photometric observations from a run have been reduced, we fit the results according to

$$m = m_1 - 2.5\log(f) - A\ \sec z + C\ (V-I), \tag{1}$$

where f is the flux from the star in terms of electrons per second. We have found that m_1 and C are constant during a run with a given CCD and filter, so we fit for a single value for these parameters and extinction coefficients A for each night. The rms residual of the fit is typically about 0.01 magnitude which is satisfactory accuracy for our purposes. Table 1 lists typical values for m_1, A, and C for each run in the two filters V and I. Note the havoc in the extinction caused by the eruption by Pinatubo in 1991.

Galaxy reductions proceed by first bias subtraction, division by a flat field, and subtraction of any fringing present in I band data. We always take multiple images of a galaxy with the telescope moved by several arcseconds between images, and determine these offsets to the nearest pixel. Any bad pixels or columns are masked out, and the images are shifted into registration. We next run a program called "autoclean" which identifies cosmic rays in the stack of images and removes them by replacement with appropriately scaled data from the rest of the stack. Autoclean also gives us an estimate of how photometric the sequence of observations was by producing accurate flux ratios between the exposures. Finally we make a mask of the obvious stars and companion galaxies in the cleaned image and determine the sky background by fitting the outer parts of the galaxy image with an $r^{1/4}$ profile plus sky level. This is usually done simultaneously for V and I images, and

when the sky levels are determined, we also compute $(V-I)_0$ colors as a function of radius from the center of the galaxy.

In order to knit all of our observations into a consistent photometric system, we attempted to make sure that there were overlap observations between runs, and we developed a pair of programs called "apphot" and "apcomp" to compare observations. "Apphot" converts a galaxy image with its photometric calibration into a table of circular aperture photometry. This only depends on plate scale (which is well known) and therefore permits comparison of different images regardless of their angular orientation. "Apcomp" then takes the aperture photometry from two observations and fits the two profiles to one another using a photometry scale offset and a relative sky level. These two programs can give us accurate offsets between the photometry of two images, good at the 0.005 magnitude level.

We learned, however, that good seeing is much more common than photometric weather, and we realized that many of our "photometric" observations were not reliable at the 0.01 magnitude level. As the survey progressed and the number of overlaps increased, we also realized that although we only need 0.05 magnitude photometry of $\overline{m}_I$, $\overline{M}_I$ is sensitive enough to $(V-I)_0$ color that we needed better photometry. The existing photoelectric (PE) photometry, although probably very good in the mean, is neither extensive enough nor accurate enough to serve to calibrate the survey.

We also became aware that there are many peculiar CCD and shutter effects which make good photometry difficult. For example, we have found photometry with Tektronix (SITe) CCDs particularly challenging for reasons we do not fully understand. Because of their high quantum efficiency and low noise they have been the detectors of choice, but run to run comparisons with apphot and apcomp show consistent zero point offsets at the 0.05 magnitude level. While not a serious problem for $\overline{m}_I$, we had to do much better in measuring $(V-I)_0$.

Accordingly, we undertook an auxiliary survey in 1995 of a substantial fraction of our SBF survey from the McGraw-Hill 1.3-m telescope at the MDM Observatory. We shared the time with another program and used only nights which were photometric, as judged by the observer at the time and as revealed later from the quality of the photometric standard observations. We did not use Tek CCDs but primarily used the front-illuminated, Loral 2048^2 CCD Wilbur (Metzger et al. 1993), we used filters which match V and I_{KC} as closely as possible, and the large field of view permitted us to make very good estimates of sky levels. Over 5 runs this comprised about 600 observations in V and I. We made certain to have a generous overlap between these observations and all our other observing runs, reaching well south to tie to the CTIO and LCO data.

We then performed a grand intercomparison of all the photometric data in order to determine photometric offsets from run to run. Using apphot and apcomp, we determined offsets between observations, and we built up a large table of comparison pairs. In addition, photoelectric (PE) photometry from deVaucouleurs and Longo (1988), Poulain and Nieto (1994), and Buta and Williams (1995) served as additional sources of comparison, and we computed differences between PE and our photometry for every galaxy in common. We have found that $(V-I)_0$ colors often show some-

what better agreement than the individual V and I measurements, presumably because thin clouds are reasonably gray, so we also compared colors directly in addition to photometric zero points.

The results are illustrated in Figure 1. In each of three quantities V, I, and $(V-I)_0$, we fitted for zero point offsets for each run (photoelectric sources were considered to be a "run"), minimizing the pairwise differences. We set the overall zero point by insisting that the median run offset be zero. Upon completion, we found that the rms of the zero point offsets to be 0.029 mag, and the rms scatter of individual comparisons between CCD data to be 0.030 mag in V, 0.026 mag in I, and 0.024 mag in $(V-I)_0$. The scatter was bigger for CCD-PE zero point comparisons, 0.047 mag in both V and I. The "zero point offsets" for the photoelectric photometry were 0.003 mag in V, 0.017 mag in I, and 0.004 mag in $(V-I)_0$, which we take to be close enough to zero that we did not choose to modify our overall median zero point to force them to zero.

Finally, we chose zero point corrections for V and I for each run according to these offsets. The difference of the corrections was set to the $(V-I)_0$ offset from the comparison, and the sum of the corrections was the sum of the V and I offsets. We therefore believe that (a) our photometry is very close to Landolt and photoelectric in zero point, (b) the error in the V or I photometry for a given observation is 0.02 mag, and (c) the error in a given $(V-I)_0$ color measurement is 0.017 mag (where we have divided by $\sqrt{2}$ to get the error for single measurements). We also add in quadrature 0.25 of the zero point offset which was applied. The offsets ΔV and ΔI for each run are listed in Table 1.

The reductions of $\overline{m}_I$ are described elsewhere (e.g., Jacoby et al. 1992). Briefly, we fit a galaxy model to the summed, cleaned, sky-subtracted galaxy image and subtract it. If there is dust present (all too common in ellipticals and S0s as well as the large bulge spiral galaxies we observe), we mask it out as well. Experiments with masking different portions of M31 and M81 (where we used B band observations to show us clearly the location of the dust) indicate that reasonable care in excising dust will produce a reliable $\overline{m}_I$, both because the extinction is less in the I band and also because the dust tends to cause structure at relatively large scales which are avoided by our fit to the Fourier power spectrum. We run DoPhot (Schechter et al. 1993) on the resulting image to find stars, globular clusters, and background galaxies; fit a luminosity function to the results; and derive a mask of objects brighter than a completeness limit and an estimate of residual variance from sources fainter than the limit. Applying the mask to the model-subtracted image, we calculate the variance from the fluctuations in a number of different regions. Finally, this variance is converted to a value for $\overline{m}_I$ by dividing by the mean galaxy flux and subtraction of the residual variance estimate from unexcised point sources. Generally speaking, the various estimates of $\overline{m}_I$ are quite consistent from region to region, and a weighted average and error estimate are tabulated for each observation. If the observation was photometric, we also record the $(V-I)_0$ color found in the same region in which we measure $\overline{m}_I$.

There are many galaxies for which $(V-I)_0$ and $\overline{m}_I$ have been measured more than once, and intercomparison of the different observations can be used to evaluate whether our error estimates are

reasonable. If we consider all pairs and divide their difference by the expected error, the distribution should be a Gaussian of unity variance. Figure 2 illustrates these distributions for $\overline{m}_I$ and $(V-I)_0$. Evidently, the error estimates are usually quite good, with discordant observations occurring rarely. In most cases of discordances, it is clear which of the observations is trustworthy, and we simply remove the other observation from further consideration. These excised observations occur 1.5% of the time for $\overline{m}_I$ and 0.3% of the time for $(V-I)_0$, and are an indication of how frequently bad observations occur.

After observations are averaged together, they are subjected to some final corrections. The mean $(V-I)$ color of the fluctuations is the mean of a galaxy's color $(V-I)$ and the "fluctuation color" $\overline{m}_V$–$\overline{m}_I$, or $(V-I) \approx 1.85$ (since the rms fluctuation is the square root of the flux from the galaxy and the flux from $\overline{m}_I$). The value of $\overline{m}_I$ is corrected according to this mean color and the color term for the run's photometry. The values of $\overline{m}_I$ and $(V-I)$ are corrected for galactic extinction according to

$$A_V : A_{I_{\rm KC}} : E(B-V) = 3.04 : 1.88 : 1.00, \tag{2}$$

where $E(B-V)$ comes from Burstein & Heiles (1984), who give $A_B = 4.0\,E(B-V)$, the relative extinction ratio $A_{I_{\rm KC}}/A_V = 0.62$ is taken from Cohen et al. (1981) for a star halfway between an A0 and an M star, and $A_V/E(B-V)$ is an adjustment of a value of 3.1 for A0 stars common in the literature (*e.g.,* Cardelli, et al. 1989) to a value of 3.04 more appropriate for early-type galaxies, following the ratios given in Cohen et al.

The final modification is the application of K-corrections which brighten magnitudes in V and I by 1.9 and $1.0 \times z$ respectively (Schneider 1996), and brighten fluctuation magnitudes in I by $7.0 \times z$ (Worthey 1996). Note that the very red color of SBF causes flux to be shifted rapidly out of the I band with redshift, but the $\overline{m}_I$ K-correction amounts to only 0.05 magnitude at a typical distance of 2000 km/s.

3. Calibrating $\overline{M}_I$

The next step we take in trying to establish how $\overline{M}_I$ varies according to stellar population is to look at how $\overline{m}_I$ varies from galaxy to galaxy within groups, where the distance to the galaxies is essentially constant. We originally chose to observe SBF in the I band because stellar population models indicate that $\overline{M}_I$ is relatively constant from population to population, and that the effects of age, metallicity, and IMF are almost degenerate — in other words, $\overline{M}_I$ is nearly a one parameter family.

Guided by theoretical models we seek to establish whether three statements are a fair description of our data:

(§3.1) $\overline{M}_I$ is a one-parameter family, with a universal dependence on $(V-I)_0$ (i.e., $\overline{M}_I$ is a function of $(V-I)_0$ with small residual scatter).

(§3.2) The zero point of the $\overline{M}_I$–$(V-I)_0$ relation is universal.

(§3.3) The $\overline{M}_I$–$(V-I)_0$ relation is consistent with theoretical models of stellar populations.

To this end we chose approximately 40 nearby groups where we currently have (or will have) observed more than one galaxy. The groups are defined by position on the sky and a redshift range and in most cases correspond to one of the groups described by Faber et al. (1989). Table 3 lists our groups. Note that we are not trying to include all groups, nor do we have to be complete in including all galaxies which are members. We are simply trying to create samples of galaxies for which we are reasonably confident that all galaxies are at the same distance.

3.1. Universality of the $\overline{m}_I$ dependence on $(V-I)_0$

Figure 3 illustrates the $\overline{m}_I$–$(V-I)_0$ relationship in six groups where we have measured SBF in a number of galaxies: NGC 1023, Leo, Ursa Major, Coma I&II, Virgo, and Fornax. The lines are drawn with slope 4.5 and zero point according to the fit to the data described below. We see that galaxies which meet the group criteria of position on the sky and redshift are consistent with the same $\overline{m}_I$–$(V-I)_0$ relationship, where the scatter reflects both the measurement error and the group depth inferred from spread across the sky. In Virgo we find NGC 4600 much brighter than the rest of the galaxies, NGC 4365 significantly fainter, and NGC 4660 (the point at $(V-I)_0 = 1.21$ and $\overline{m}_I = 28.9$) also with an unusually bright $\overline{m}_I$ for its color. These three galaxies, marked as smaller, square symbols, are discussed below.

Note that ellipticals and S0 galaxies are intermixed with spirals (NGC 3368 in Leo, NGC 4548 in Virgo, NGC 891 in the NGC 1023 group, and NGC 4565 and NGC 4725 in the Coma I&II group). The two galaxies in Fornax marked as "spiral" (NGC 1373 and NGC 1386) might better be classified as S0 on our deep CCD images. For this admittedly small sample we see no offset between SBF measurements in spiral bulges and early-type galaxies. We regard this as confirmation of our assumption that SBF measurements are equally valid in spiral bulges as in early-type galaxies.

In order to test the hypothesis that $\overline{M}_I$ has a universal dependence on $(V-I)_0$ in a more systematic way than fitting individual groups, we simultaneously fit all our galaxies which match the group criteria with

$$\overline{m}_I = \langle \overline{m}_I^0 \rangle_j + \beta\,[(V-I)_0 - 1.15], \tag{3}$$

where we fit for values of $\langle \overline{m}_I^0 \rangle_j$ for each of j=1,N groups and a single value for β. The quantity $\langle \overline{m}_I^0 \rangle_j$ is the group mean value for $\overline{m}_I$ at a fiducial galaxy color of $(V-I)_0 = 1.15$. The measurements of $(V-I)_0$ and $\overline{m}_I$ carry errors which the pair-wise comparisons and the averaging procedure of section 2 indicate are accurate.

We also anticipate that there will be an irreducable "cosmic" scatter in $\overline{M}_I$. Accordingly, in fitting $\overline{m}_I$ as a function of $(V-I)_0$, we include an error allowance for this cosmic scatter which is nominally 0.05 magnitudes (i.e. for this fit the error in $\overline{m}_I$ is enhanced by 0.05 magnitude in

quadrature). In addition, we will also see scatter because the galaxies within groups are not truly at the same distance. We therefore calculate the rms angular position of the galaxies making up each group, and divide this radius by $\sqrt{2}$ as an estimate of the rms group depth. Converting this to a magnitude, we add it in quadrature to the error in $\overline{m}_I$. We then perform a linear fit of $N+1$ parameters which allows for errors in both the ordinate and abcissa, according to the "least distance" method used by Tonry and Davis (1981). (This also appears in a slightly different guise in the second edition of *Numerical Recipes* by Press et al. 1992)

We remove the three Virgo galaxies which we believe are at significantly different distances from the rest of the group (NGC 4365, NGC 4660, and NGC 4600), mindful that what is considered to be part of Virgo and what is not is somewhat arbitrary. We also choose to exclude NGC 205 and NGC 5253 from the fit because recent starbursts make them extremely blue — we do not believe our modeling extends to such young populations.

With 149 galaxies we have 117 degrees of freedom, and we find that $\chi^2 = 129$, $\chi^2/N = 1.10$, and the slope of the $\overline{M}_I$–$(V-I)_0$ relation is 4.5 ± 0.25. The galaxies contributing to the fit span a color range of $1.0 < (V-I)_0 < 1.3$. Because Virgo still contributes five of the seven most discrepant points (the other two are in Cetus), the rms depth used for Virgo ($2.35^\circ \rightarrow 0.08$ mag) may be too small, making χ^2/N slightly bigger than one. If we replace the 3 Virgo galaxies we omitted earlier, we find that χ^2/N rises to 1.75 for 120 degrees of freedom and the slope changes to 4.7 ± 0.25, showing that even though these galaxies are significantly outside of Virgo, the slope is robust. When we experiment with adding and removing different groups we find that the slope changes slightly, but is always consistent with the error above.

These values for χ^2 include an allowance for cosmic scatter of 0.05 magnitude and the nominal, rms group depth. These two, ill-constrained sources of error can play off against each other: if we double the group depth error allowance, we get $\chi^2/N = 1.0$ for zero cosmic scatter; if we increase the cosmic scatter to 0.10 magnitude, we need to decrease the group depth to zero in order to make $\chi^2/N = 1.0$. Therefore, even though we cannot unambiguously determine how much cosmic scatter there is in the $\overline{M}_I$–$(V-I)_0$ relation, it appears to be $\sim$0.05 mag.

The referee pointed out that even if we make no allowance for group depth, the cosmic scatter of 0.10 mag makes SBF the most precise tertiary distance estimator by far, and wanted to know how sensitive this is to our estimates of observational error. There is not much latitude for the cosmic scatter to be larger than 0.10 mag. The distribution of measurement error in $\overline{m}_I$ and $(V-I)_0$ (which also enter χ^2) starts at 0.06 mag, and has quartiles at 0.11, 0.16, and 0.20 mag. If we wanted to increase the cosmic scatter by $\sqrt{2}$ to 0.14 mag, we would have to have overestimated the observational errors by 0.10 mag in quadrature, and apart from the fact that a quarter of the measurements would then have imaginary errors, our pairwise comparison of multiple observations from the previous section would not allow such a gross reduction in observational error.

Figure 4 illustrates how $\overline{m}_I$ depends on $(V-I)_0$ when all the group data have been slid together by subtraction of the group mean at $(V-I)_0 = 1.15$. Note again that spiral galaxies, in this case

four galaxies with both Cepheid and SBF distances, show no offset relative to the other early-type galaxies making up the groups in which they appear, other than the usual trend with $(V-I)_0$. The overall rms scatter, 0.18 mag, arising from all the effects discussed above, is a testament to the quality of SBF as a distance estimator.

The Local Group galaxies NGC 205, NGC 147, and NGC 185 have also been plotted in Figure 4 (although they were not used in the fit), under the assumption that they are at the same distance as M31 and M32. This may or may not be a valid assumption for NGC 147 and NGC 185, but they agree reasonably well with the mean relation. In contrast to these two galaxies, which are blue because of extremely low metallicity, NGC 205 has undergone a recent burst of star formation and has a strong A star spectral signature. Because our models do *not* extend to such young populations, the systematic deviation from the mean relation is not unexpected.

The inset in Figure 4 extends the color range to show that this deviation continues for two other galaxies where there has been recent star formation: NGC 5253 and IC 4182. NGC 5253 is 0.5 mag fainter than one would expect using a naive extrapolation of the relation to its color of $(V-I)_0 = 0.84$, and IC 4182 has an SBF magnitude which is 0.75 mag fainter than one would judge from its Cepheid distance and its color of $(V-I)_0 = 0.71$. Qualitatively this makes sense because the very young stars change the overall color of the galaxy quite a bit but are not very luminous in the I band compared to the stars at the top of the RGB which are the main contributors to the SBF $\overline{m}_I$. It may be that these very young populations can be understood well enough that one can safely predict the SBF absolute magnitude from the mean color, but this is beyond the scope of this paper.

Tammann (1992) expressed concern that there are residual stellar population effects in SBF even after the correction for $(V-I)_0$ color. However, his critique was based on an early attempt to correlate $\overline{m}_I$ as a function of $(V-I)_0$ (Tonry et al. 1990). Unfortunately, that work had the wrong sign for the slope (appropriate for the JHK bandpasses but not I), because it was based on the Revised Yale Isochrones (Green et al. 1987), which did not properly model the line blanketing in metal rich, high luminosity stars. The effect noted by Tammann was a residual correlation of the corrected $\overline{m}_I^0$ with the Mg_2 index among galaxies within a cluster. Figure 5 shows these trends do not exist for the present data and the new $\overline{m}_I$–$(V-I)_0$ relation: in both Fornax and Virgo there is no residual correlation with either Mg_2 or galaxy magnitude.

We conclude that a one-parameter, linear relation between $\overline{M}_I$ and $(V-I)_0$ suffices to describe our data for $1.0 < (V-I)_0 < 1.3$; the slope of the $\overline{M}_I$–$(V-I)_0$ relation is universally 4.5 ± 0.25, and we are indeed detecting cosmic scatter in $\overline{M}_I$ of order 0.05 mag. Very few galaxies fail to follow the relation, and for every such galaxy at least one of the following statements is true: (1) the measurement of $\overline{m}_I$ or $(V-I)_0$ is doubtful; (2) the galaxy may not be a member of the group we assigned it to; (3) the stellar population is bluer than $(V-I)_0 = 1.05$ due to recent star formation.

Note that this slope is steeper than the value of 3 tendered by Tonry (1991) and used by Ciardullo et al. (1993) who suggested that it might be as steep as 4. Basically, the reason for this

is that the older data were noiser and were fitted only to errors in the ordinate, whereas in fact the errors in $(V-I)_0$ are quite significant, particularly for the better measured $\overline{m}_I$, which count heavily in any weighted fit.

3.2. Universality of the $\overline{M}_I$ zero point

We have effectively tested the hypothesis that the zero point of SBF is universal within groups, but in order to extend the test from group to group we need independent distance estimates. Since the groups are all nearby, the group's redshift is not an accurate distance estimate — there are likely to be substantial non-Hubble velocities included in the group's recession velocity. We therefore turn to other distance estimators: Cepheids, planetary nebula luminosity function (PNLF), Tully-Fisher (TF), $D_n-\sigma$, Type II supernovae (SNII) and Type I supernovae (SNIa). Some of these estimators have zero points in terms of Mpc (such as Cepheids and SNII), others have zero points in terms of km/s based on the Hubble flow (such as $D_n-\sigma$), and a few have both (such as TF). For our initial discussion we seek only to establish whether the relative distances agree with SBF; for now we do not care about the zero point, though it will soon be addressed.

Figures 6 and 7 show the comparison between the values of the SBF parameters $\langle\overline{m}_I^0\rangle$ derived previously for each of our groups and the distances to the groups according to these 6 methods. The results of fitting lines of unity slope (allowing for errors in both coordinates) to the data in each panel are given in Table 4. We use the published error estimates for all of these other indicators so χ^2/N should be viewed with some caution: outliers and non-Gaussian errors or over-optimistic error estimates can inflate χ^2/N even though the mean offset is still valuable. Since each comparison is very important, we briefly discuss them individually.

3.2.1. Cepheids

There is now a growing number of Cepheid distances with which we compare, but we are faced with the complication that Cepheids occur in young stellar populations, while SBF is best measured where such populations are not present.

There are five galaxies which have both Cepheid and SBF distances: NGC 224 (Freedman & Madore 1990), NGC 3031 (Freedman et al 1994), NGC 3368 (Tanvir et al. 1995), NGC 5253 (Saha et al. 1995), and NGC 7331 (Hughes 1996). NGC 5253 is especially problematic for SBF, because its recent starburst has produced a much younger and bluer stellar population than we have calibrated. We can, of course, also compare distances according to group membership. There are 7 groups where this is currently possible: Local Group, M81, CenA, NGC 1023 (NGC 925 from Silbermann et al. 1996), NGC 3379 (also including NGC 3351 from Graham et al. 1996), NGC 7331, and Virgo (including NGC 4321 from Ferrarese et al. 1996, NGC 4536 from Saha et al. 1996a, and NGC 4496A from Saha et al. 1996b; we exclude NGC 4639 from Sandage et al. 1996

because we are also excluding NGC 4365 and the W cloud from the SBF mean). In the former case we find that fitting a line to $\langle \overline{m}_I^0 \rangle$ as a function of $(m-M)$ yields a mean offset of -1.75 ± 0.05 mag with χ^2/N of 3.4 for 4 degrees of freedom, and -1.82 ± 0.06 mag with χ^2/N of 0.3 for 3 degrees of freedom when NGC 5253 is excluded. In the latter case we get a mean offset of -1.74 ± 0.05 mag with χ^2/N of 0.6 for 6 degrees of freedom. When NGC 5253 is excluded, the rms scatter is remarkably small, only 0.12 magnitudes for the galaxy comparison and 0.16 magnitudes for the group comparison.

3.2.2. PNLF

Ciardullo et al. (1993) reported virtually perfect agreement between SBF and PNLF, but recent publications (Jacoby et al. 1996) have raised some discrepancies. Examination of Figure 7 reveals that our fit has two outliers: Coma I (e.g. NGC 4278) and Coma II (e.g. NGC 4494). Because we do not know how to resolve this issue at present, Table 4 gives the result for $\langle \overline{m}_I^0 \rangle - (m-M)_{\rm PNLF}$ for the entire sample and when these two outliers are removed. Since PNLF is fundamentally calibrated on Cepheids, this is not independent of the previous number, but it does confirm that PNLF and SBF are measuring the same relative distances.

3.2.3. SNII

The expanding photospheres method (EPM) described most recently by Eastman et al. (1996) offers distance estimates which are largely independent of the Cepheid distance scale. There is only one galaxy with both an EPM and an SBF distance (NGC 7331), but there have also been two SNII in Dorado (NGC 1559 and NGC 2082), two in Virgo (NGC 4321 and NGC 4579), and one in the NGC 1023 group (NGC 1058). The agreement between EPM and SBF (Fig. 6) is good. The farthest outlier is NGC 7331, for which SBF and Cepheid distances are discordant with the SNII distance. Table 4 lists separately the zero point, scatter, and χ^2/N when NGC 7331 is included and excluded.

3.2.4. TF (Mpc calibration)

B. Tully (1996) was kind enough to provide us with TF distances to the SBF groups in advance of publication. The fit between TF and SBF gives $\langle \overline{m}_I^0 \rangle - (m-M) = -1.69 \pm 0.03$ mag. This is again not independent of the Cepheid number, since the TF zero point comes from the same Cepheid distances. Figure 7 demonstrates that the agreement is generally good, despite the high χ^2/N which comes from a few non-Gaussian outliers. We cannot tell whether these outliers reflect non-Gaussian errors in the methods or simply the difficulties of choosing spirals and early type galaxies in the same groups.

3.2.5. TF (km/s calibration)

We applied the SBF group criteria to the "Mark II" catalog of galaxy distances distributed by D. Burstein. We selected all galaxies with "good" TF distances (mostly from Aaronson et al. 1982) and computed an average distance to the groups, applying the usual Malmquist bias correction according to the precepts of Lynden-Bell et al. (1988) and the error estimates from Burstein. Because these distances have a zero point based on the distant Hubble flow, we derive an average offset of $\langle \overline{m}_I^0 \rangle \ - 5 \log d = 13.55 \pm 0.08$ mag.

3.2.6. D_n–σ

Most of the SBF groups are the same as those defined by Faber et al. (1989). We compare their Malmquist bias corrected distances to these groups (which are based on a zero point from the distant Hubble flow) with SBF and find the same result as Jacoby et al. (1992): the distribution of errors has a larger tail than Gaussian, but the error estimates accurately describe the central core of the distribution. χ^2/N is distinctly larger than 1, but the difference histogram in Figure 7 reveals that this is because of the tails of the distribution. The fit between D_n–σ and SBF gives $\langle \overline{m}_I^0 \rangle \ - 5 \log d = 13.64 \pm 0.05$ mag.

3.2.7. SNIa

Extraordinary claims have been made recently about the quality of SNIa as distance estimators. Some authors (e.g. Sandage and Tammann 1993) claim that suitably selected ("Branch normal") SNIa are standard candles with a dispersion as little as 0.2 mag. Others (e.g. Phillips 1993) believe that they see a correlation between SNIa luminosity and their rate of decline, parametrized by the amount of dimming 15 days after maximum, Δm_{15}. Still others (e.g. Riess et al. 1995) agree with Phillips (1993) but believe that they can categorize SNIa better by using more information about the light curve shape than just this rate of decline. Finally, there is the "nebular SNIa method" of Ruiz-Lapuente (1996) which tries to determine the mass of the exploding white dwarf by consideration of the emission lines from the expanding ejecta. We therefore choose to compare SBF distances with SNIa under two assumptions: that SNIa are standard candles, and that $m_{max} - \alpha \Delta m_{15}$ is a better indicator of distance. In both cases we restrict our fits to $0.8 < \Delta m_{15} < 1.5$ as suggested by Hamuy et al. (1995) and use a distance error of 0.225 mag for each SNIa.

SNIa have been carefully tied to a zero point according to the distant Hubble flow (one of the main advantages of SNIa) by Hamuy et al. (1995), under both assumptions. There have also been vigorous attempts to tie the SNIa to the Cepheid distance scale which we have chosen not to use because of the circularity with our direct comparison between SBF and Cepheids.

The results are both encouraging and discouraging. We find that there is indeed a good

correlation between SNIa distance and SBF, with average values of $\langle \overline{m}_I^0 \rangle - 5 \log d = 13.92 \pm 0.08$ mag and 14.01 ± 0.08 mag for the group comparison under the two assumptions. As illustrated in Figure 6, $m_{max} - \alpha \Delta m_{15}$ does correlate better with distance than m_{max}, but as long as "fast declining" SNIa are left out there is scant difference between the zero point according to the two methods.

The panels of Figure 6 showing SBF and SNIa hint at a systematic change between the nearest three and the farthest three groups, in the sense that there appears to be a change in zero point by about 0.7 mag. One might worry that this is evidence that SBF is "bottoming out", but there is no hint of this in the comparisons with TF and $D_n - \sigma$ in Figure 7 which extend to much fainter $\overline{m}_I$. One might also worry about whether there are systematic differences in SNIa in spirals and ellipticals, and biases from the lack of nearby ellipticals or S0 galaxies. However, it is probably premature to examine these points in too much detail. For example, the point at $\langle \overline{m}_I^0 \rangle \approx 28$ uses the SBF distance to Leo I, but the SNIa occurred in NGC 3627 which lies 8° away from the Leo I group. This is a fundamental difficulty in the SBF–SNIa comparison, which will improve as SBF extends to greater distances and more nearby SNIa are observed.

There are seven galaxies bearing SNIa where SBF distances have been measured: NGC 5253 (SN 1972E), NGC 5128 (SN 1986G), NGC 4526 (SN 1994D), NCG 2962 (SN 1995D), NGC 1380 (SN 1992A), NGC 4374 (SN 1991bg), NGC 1316 (SN 1980N). Inasmuch as two of these are slow decliners (SN 1986G, SN 1991bg), we fit the remaining five using the SBF distance to the galaxy instead of the group. We derive $\langle \overline{m}_I^0 \rangle - 5 \log d = 13.86 \pm 0.12$ mag and 14.01 ± 0.12 mag for the two methods.

We regard the SBF distance to NGC 5253 as uncertain because we have not calibrated $\overline{M}_I$ for such a young stellar population. We thus also recompare SBF and SNIa with NGC 5253 removed from consideration. χ^2/N becomes dramatically smaller in both cases and $\langle \overline{m}_I^0 \rangle - 5 \log d$ become smaller by about 0.2 mag to 13.64 ± 0.13 mag and 13.87 ± 0.13 mag.

3.2.8. Zero point summary

These comparisons demonstrate that the second hypothesis is correct: the zero point of the $\overline{M}_I$–$(V-I)_0$ relationship is universal. We use the SBF–Cepheid fit to derive a final, empirical relationship between $\overline{m}_I$ and $(V-I)_0$:

$$\overline{M}_I = (-1.74 \pm 0.07) + (4.5 \pm 0.25)\,[(V-I)_0 - 1.15]. \tag{4}$$

This zero point differs from that of Tonry (1991) by about 0.35 magnitude. The reason is simply that the 1991 zero point was based entirely on M31 and M32, and the observational error in both $\overline{m}_I$ and $(V-I)_0$ worked in the same direction, as did the photometric zero point errors (cf. Table 1 for K0990). The SBF distances which have been published therefore increase by about 15 percent (for example Fornax moves from 15 Mpc to 17 Mpc), except for Virgo, where

the earlier result included NGC 4365 which we now exclude in calculating the average distance to the core of the cluster. This new calibration is based on 10 Cepheid distances in 7 groups and 44 SBF distances. As seen in Figure 6 and Table 4, these are highly consistent with one another with a scatter of about 0.15 mag. Along with the extensive photometric recalibration, this zero point should be accurate to ± 0.07 mag. This error estimate makes an allowance of 0.05 mag for the uncertainty in the Cepheid zero point in addition to the statistical error of 0.05 mag, and the comparisons with theory and SNII give us confidence that this truly is correct.

3.3. Comparison with theory

Finally we test our third hypothesis by comparing our $\overline{M}_I$–$(V-I)_0$ relationship with theoretical models of stellar populations. Figure 8 shows the model predictions of Worthey (1993a,b) along with the empirical line. When the theoretical models are fitted with the empirically determined slope of 4.5, they yield a theoretical zero point of -1.81 mag with an rms scatter of 0.11 mag for the SBF relation. We enter this value in Table 4, with the scatter offered as an "error estimate", but it must be remembered that this is fundamentally different from the other entries in the table. There is good agreement here, although the theoretical result for $\overline{M}_I$ may be slightly brighter (0.07 mag) or slightly redder (0.015 mag) than the empirical result. Given the difficulties that the theoretical models have in simultaneously fitting the color and Mg_2 indices of real galaxies, we regard this agreement as excellent confirmation of the empirical calibration.

4. The Hubble Constant

The scope of this paper does not extend to comparing SBF distances with velocity; this will be the subject of the next paper in the series. However, the comparison with other distance estimators does provide us with a measurement of the Hubble constant.

The comparison with other estimators whose zero point is defined in terms of Mpc tells us the absolute magnitude of SBF. At our fiducial color of $(V-I)_0 = 1.15$, we find that Cepheids give us an absolute magnitude $\overline{M}_I = -1.74 \pm 0.05$. We prefer the group-based Cepheid comparison because of the very few SBF measurements possible in spirals which have Cepheids. The other Mpc-based distance estimators are all consistent with this zero point, as we would hope since they are calibrated with the same Cepheid data. The results from theoretical models of stellar populations and SNII are also consistent with this zero point, and provide independent confirmation of the validity of the Cepheid distance scale.

The comparison of SBF with estimators whose zero point is based on the large scale Hubble flow is less consistent. The estimators based on galaxy properties, TF and D_n–σ, are consistent with one another and consistent with SBF in terms of relative distances. They give a zero point for SBF at the fiducial color of $(V-I)_0 = 1.15$ of $\langle \overline{m}_I^0 \rangle = 5 \log d(\mathrm{km/s}) + 13.59 \pm 0.07$, where the

error comes from the rms divided by $\sqrt{N-1}$.

Supernovae and SBF are more interesting. The group membership of the Cepheid galaxies was not difficult since they were specifically chosen to be group members. In contrast, the SNIa are not easy to assign to groups in many cases. Depending on (1) whether we fit galaxies individually or groups, (2) whether we use the "standard candle" model for SNIa or the "light curve decline" relation, and (3) whether we include or exclude NGC 5253 for which we regard our stellar population calibration as unknown, we get values for the SBF zero point as low as 13.64 and as high as 14.01 (Table 4). Averaging the two methods and again estimating uncertainties from rms divided by $\sqrt{N-1}$, we find 13.96 ± 0.17 for groups and 13.75 ± 0.14 for galaxies. Because these differ from the TF and $D_n{-}\sigma$ by 2.0 σ and 1.0 σ respectively, the discrepancy may not be statistically significant.

It is possible that there are systematic errors in the tie to the distant Hubble flow for TF and $D_n{-}\sigma$, whereas the SNIa appear to be wonderfully consistent with the large scale Hubble flow. On the other hand, the nearby SNIa do not agree with SBF or Cepheids as well as one might hope from the scatter against the Hubble flow, which makes one worry about the systematics with SN1a. For example, the SN1a distances predicted for the Fornax clusters are significantly larger than the very recent Cepheid measurement of the distance to the Fornax cluster (Silbermann et al. 1996b). SNII appear to agree pretty well with SBF and Cepheids, and there should eventually be enough of them to tie very well to the large scale Hubble flow. In subsequent papers we will present the direct tie between SBF and the Hubble flow, both from ground-based observations as well as HST observations beyond 5000 km/s, but at present we depend on these other estimators to tie to the Hubble flow. It is therefore with some trepidation that we offer a value for H_0.

We have a calibration for $\overline{M}_I$; we have several calibrations for $\overline{m}_I$ in terms of $5 \log d(\mathrm{km/s})$; and of course $(m{-}M) = 5 \log d(\mathrm{km/s}) + 25 - 5 \log H_0$. If we use the TF and $D_n{-}\sigma$ calibration of SBF we get $H_0 = 86$ km/s/Mpc. Examining groups and averaging the "standard candle" and the "Δm_{15}" assumptions about SNIa gives us $H_0 = 72$ km/s/Mpc. If we compare galaxies directly without resorting to group membership, but leave out NGC 5253, we get an average $H_0 = 80$ km/s/Mpc.

We suspect that there is more to the SNIa story than is currently understood, so we therefore prefer not to use it to the exclusion of all other distance estimators. The range we find for H_0 is

$$H_0 = 72 - 86 \text{ km/s/Mpc},$$

and our best guess at this point is derived by averaging the ties to the Hubble flow from TF, $D_n{-}\sigma$, SNIa (both methods) in groups and SNIa (both methods) galaxy by galaxy. This weights the SNIa slightly more heavily than TF and $D_n{-}\sigma$ and gives a zero point of 13.72 which translates to

$$H_0 = 81 \pm 6 \text{ km/s/Mpc}.$$

The final error term includes a contribution of 0.07 magnitude from the disagreement between the Cepheid and theory zero points (which we hope is indicative of the true accuracy of our calibrations), and an allowance of 0.13 magnitude for the uncertainty in the tie to the distant Hubble flow (judged from the scatter among the various methods).

In order to facilitate comparisons with SBF distances, we offer the SBF distance to 12 nearby groups in Table 5. The relative distances are completely independent of any other distance estimator, and the zero point uses our Cepheid-based calibration. As we finish our reductions and analysis, the remainder of the group and individual galaxy distances will be published.

5. Summary and Conclusions

We have described the observational sample which comprises the SBF Survey of Galaxy Distances. The survey was conducted over numerous observing runs spanning a period of nearly seven years. The photometry of the sample has been brought into internal consistency by applying small systematic corrections to the photometric zero points of the individual runs. Based on comparisons between overlapping galaxy observations, we find that our error estimates for $(V-I)$ and $\overline{m}_I$ are reliable, after correction for the photometry offsets.

From our measurements of $\overline{m}_I$ within galaxy groups, we conclude that $\overline{M}_I$ is well described by a linear function of $(V-I)_0$. Comparison of our relative distances with Cepheid distances to these groups indicates that this linear relationship is universal and yields the zero point calibration for the SBF method. This calibration is applicable to galaxies that are in the color range $1.0 < (V-I)_0 < 1.3$ and which have not experienced recent bursts of star formation. Any intrinsic, or "cosmic," scatter about this relation is small, of order 0.05 mag. Owing to many more data and improved photometry, this new calibration differs in its zero point by 0.35 mag from the earlier one of Tonry (1991), but is much closer to Worthey's (1993) theoretical zero point, differing by just 0.07 mag. We take this close agreement to be an independent confirmation of the Cepheid distance scale.

An extensive set of comparisons between our SBF distances and those estimated using other methods provides still further evidence for the universality of the $\overline{M}_I$–$(V-I)_0$ relation. We find that the various methods are all generally quite reliable, apart from occasional outliers which serve to inflate the χ^2 values for the comparisons. Coupled with our distance zero point, our comparisons with methods tied to the distant Hubble flow yield values of H_0 in the range 72–86 km/s/Mpc. The comparison with SNIa suggests values between 72 and 80, and D_n–σ and TF call for values around 86. Thus, the controversy over H_0 continues, but the famous "factor of two" is now a factor of 20 percent.

Although the SBF Survey is still a work in progress, it is near enough to completion that the calibration presented in this paper should not change in any significant way. Future papers in this series will use the SBF survey distances to address such issues as the velocity field of the Local Supercluster and a direct determination of H_0, bulk flows, the Great Attractor, and the specific details of our SBF analysis method, including comprehensive listings of our $(V-I)_0$ and distance measurements for individual galaxies.

We would like to thank many people for collecting SBF and photometry observations for us: Bob Barr, Andre Fletcher, Xiaohui Hui, Gerry Luppino, Mark Metzger, Chris Moore, and Paul Schechter. This research was supported by NSF grant AST-9401519, and AD acknowledges the support of the National Science Foundation through grant AST-9220052.

Table 1. Observing Runs.

Run	Telescope	CCD	$''/p$	m_{1V}	A_V	C_V	ΔV	m_{1I}	A_I	C_I	ΔI
K0389	KPNO4m	TI-2	0.299	26.15	0.150	−0.070	0.014	25.42	0.070	0.000	0.012
M1189	MDM2.4m	ACIS	0.465	23.47	0.179	0.013	0.000	22.44	0.065	0.000	0.000
C0990	CTIO4m	TI	0.299	26.23	0.160	0.0	−0.026	25.29	0.080	0.0	−0.003
K0990	KPNO4m	TI-2	0.299	26.26	0.160	0.0	0.019	25.39	0.080	0.0	0.045
H0291	CFH3.6m	SAIC	0.131	24.86	0.089	0.0	−0.016	24.62	0.033	0.0	0.029
L0391	LCO2.4m	Tek	0.229	24.92	0.15	0.0	0.024	24.62	0.07	0.0	0.030
C0491	CTIO4m	Tek1	0.472	26.06	0.16	0.0	0.069	26.02	0.11	0.0	0.061
K0691	KPNO4m	TI-2	0.300	25.97	0.155	0.0	−0.002	25.36	0.06	0.0	0.019
C1091	CTIO4m	Tek2	0.472	26.21	0.45	−0.007	0.019	26.08	0.3	0.025	0.040
H1091	CFH3.6m	SAIC	0.131				0.000	24.62	0.07	0.0	0.000
L1191	LCO2.4m	Tek	0.229	24.92	0.15	0.0	0.034	24.62	0.07	0.0	−0.014
M1191	MDM2.4m	ACIS	0.257	25.11	0.205	0.0	−0.025	24.53	0.102	0.035	0.007
C0492	CTIO4m	Tek2	0.472	26.05	0.220	0.005	0.014	25.93	0.145	0.030	−0.020
M0492	MDM2.4m	Lorl	0.343	24.69	0.33	0.000	0.010	24.84	0.20	0.045	0.007
H0592	CFH3.6m	STIS	0.152	25.91	0.210	0.0	−0.010	25.60	0.110	0.0	−0.038
M0892	MDM2.4m	Lorl	0.343	24.64	0.254	0.000	0.000	24.74	0.145	0.045	0.000
L1092	LCO2.4m	Tek	0.229	24.92	0.15	0.0	0.000	24.62	0.07	0.0	0.000
M1092	MDM2.4m	Lorl	0.343	24.68	0.32	0.000	0.010	24.82	0.22	0.046	0.029
L0493	LCO2.4m	Tek	0.229	24.92	0.15	0.0	0.027	24.62	0.07	0.0	−0.070
M0493	MDM2.4m	Lorl	0.343	24.67	0.21	0.022	−0.004	24.35	0.13	0.030	0.014
M0493	MDM2.4m	Tek	0.275	25.32	0.24	0.005	−0.004	24.60	0.11	0.012	0.014
M0593	MDM2.4m	Lorl	0.343	24.70	0.22	0.022	−0.033	24.35	0.138	0.030	−0.009
M0593	MDM2.4m	Tek	0.275	25.32	0.198	0.025	−0.033	24.74	0.134	0.030	−0.009
M0893	MDM2.4m	Lorl	0.343	24.82	0.19	0.012	−0.021	24.54	0.10	0.025	−0.006
M0294	MDM2.4m	Tek	0.275	25.11	0.150	−0.017	−0.040	24.84	0.058	0.015	−0.074
L0394	LCO2.4m	Tek	0.229	24.92	0.15	0.0	0.026	24.62	0.07	0.0	−0.030
L0994	LCO2.4m	Tek	0.229	24.92	0.15	0.0	0.016	24.62	0.07	0.0	0.022
G0395	MDM1.3m	Lorl	0.637	23.22	0.15	0.019	−0.029	22.84	0.064	0.026	−0.007
G0495	MDM1.3m	Lorl	0.637	23.15	0.15	0.015	−0.041	22.83	0.064	0.010	−0.012
G0495	MDM1.3m	STIS	0.445	23.11	0.15	0.015	−0.041	22.65	0.100	0.010	−0.012
G0695	MDM1.3m	Lorl	0.637	23.13	0.15	0.042	−0.015	22.79	0.061	0.026	0.000
G0995	MDM1.3m	Lorl	0.637	22.97	0.14	0.014	−0.009	22.81	0.05	0.026	−0.015
G1095	MDM1.3m	STIS	0.445	22.98	0.15	0.005	−0.015	22.70	0.06	0.008	−0.015
M0295	MDM2.4m	Tek	0.275	25.11	0.150	−0.014	−0.040	24.84	0.058	0.012	−0.074
M0395	MDM2.4m	Tek	0.275	25.11	0.150	−0.017	−0.040	24.84	0.058	0.015	−0.074
L0495	LCO2.4m	Tek	0.229	24.92	0.15	0.0	0.008	24.62	0.07	0.0	−0.027
L1095	LCO2.4m	Tek	0.229	24.92	0.15	0.0	0.000	24.62	0.07	0.0	0.000
M1295	MDM2.4m	Tek	0.275	25.11	0.150	−0.017	−0.040	24.84	0.058	0.015	−0.074
M0196	MDM2.4m	Tek	0.275	25.11	0.150	−0.017	−0.040	24.84	0.058	0.015	−0.074
M0396	MDM2.4m	Tek	0.275	25.11	0.150	−0.017	−0.040	24.84	0.058	0.015	−0.074

Note. — Columns: Run name, telescope, detector, plate scale ($''$/pixel), photometric zero point, extinction, color term, and run offset for the V band then I band.

Table 2. Landolt Fields.

Field	RA	Dec	V_{min}	V_{max}	$(V-I)_{min}$	$(V-I)_{max}$
SA92-250	00 54 41	+00 41 11	14.09	15.35	0.67	1.34
SA95-190	03 53 16	+00 16 25	12.63	14.34	0.42	1.37
SA95-275	03 54 40	+00 27 24	12.17	14.12	1.40	2.27
SA98-650	06 52 11	−00 19 23	11.93	13.75	0.17	2.09
Rubin-149	07 24 13	−00 31 58	11.48	13.87	−0.11	1.13
PG0918+029	09 21 36	+02 47 03	12.27	14.49	−0.29	1.11
PG1323−085	13 25 44	−08 49 16	12.08	14.00	−0.13	0.83
PG1633+099	16 35 29	+09 46 54	12.97	15.27	−0.21	1.14
SA110-232	18 40 50	+00 01 51	12.52	14.28	0.89	2.36
SA110-503	18 43 05	+00 29 10	11.31	14.20	0.65	2.63
Markarian-A	20 43 59	−10 47 42	13.26	14.82	−0.24	1.10

Note. — Columns: Field name, J2000 coordinates, V magnitude of the brightest and faintest star, and the $(V-I)$ colors of the bluest and reddest star.

Table 3. Nearby SBF Groups.

Group	Example	RA	Dec	rad	v_{ave}	v_{min}	v_{max}	7S#
LocalGroup	N0224	10.0	41.0	5	−300	−500	−100	282
Cetus	N0636	24.2	−7.8	10	1800	1500	2000	26
N1023	N1023	37.0	35.0	9	650	500	1000	
N1199	N1199	45.3	−15.8	2	2700	2500	3000	29
Eridanus	N1407	53.0	−21.0	6	1700	500	2300	32
Fornax	N1399	54.1	−35.6	6	1400	500	2100	31
Dorado	N1549	63.7	−55.7	5	1300	700	1700	211
N1700	N1700	72.2	−3.5	3	4230	3600	4500	100
N2768	N2768	136.9	60.2	4	1360	1100	1700	215
M81	N3031	147.9	69.3	8	−40	−200	400	
N3115	N3115	150.7	−7.5	8	700	100	900	
LeoIII	N3193	153.9	22.1	3	1400	1000	1700	45
LeoI	N3379	161.3	12.8	2	900	500	1200	57
LeoII	N3607	168.6	18.3	3	950	650	1500	48
N3640	N3640	169.6	3.5	2	1300	1200	1800	50
UMa	N3928	180.0	47.0	8	900	700	1100	
N4125	N4125	181.4	65.5	3	1300	1000	1700	54
VirgoW	N4261	184.2	6.1	2	2200	2000	2800	
ComaI	N4278	184.4	29.6	3	1000	200	1400	55
CVn	N4258	185.0	44.0	7	500	400	600	
N4386	N4386	185.6	75.8	5	1650	1500	2100	98
N4373	N4373	185.7	−39.5	2	3400	2500	3800	35
Virgo	N4486	187.1	12.7	10	1150	−300	2000	56
ComaII	N4494	187.2	26.1	5	1350	1200	1400	235
N4594	N4594	189.4	−11.4	5	1100	900	1200	
M51	N5194	200.0	45.0	4	480	380	580	
Centaurus	N4696	191.5	−41.0	3	3000	2000	5000	58
CenA	N5128	200.0	−39.0	15	550	200	600	226
N5322	N5322	212.5	57.0	6	2000	1600	2400	245
N5638	N5638	216.0	3.5	3	1650	1400	1900	68
N5846	N5846	226.0	1.8	2	1700	1200	2200	70
N5898	N5898	228.8	−23.9	2	2100	2000	2700	71
N6684	N6684	281.0	−65.2	10	850	500	1200	78
N7144	N7144	327.4	−48.5	6	1900	1500	2000	84
N7180	N7180	329.9	−20.8	10	1500	1300	1900	265
N7331	N7457	338.7	34.2	9	800	800	1100	

Table 3—Continued

Group	Example	RA	Dec	rad	v_{ave}	v_{min}	v_{max}	7S#
Grus	I1459	343.6	−36.7	5	1600	1400	2300	231

Note. — Columns: Group name, sample member, RA and Dec (B1950), group radius (deg), mean heliocentric velocity, minimum and maximum velocities for inclusion in the group, and group number from Faber et al. (1989)

Table 4. Distance Comparisons.

Estimator	Grp/gxy	Distance	N	$\langle\overline{m}_I^0\rangle - d$	$\pm$	rms	χ^2/N	Comments
Cepheid	Grp	(m-M)	7	−1.74	0.05	0.16	0.6	
Cepheid	gxy	(m-M)	5	−1.75	0.06	0.33	3.4	
Cepheid	gxy	(m-M)	4	−1.82	0.07	0.12	0.3	less N5253
PNLF	Grp	(m-M)	12	−1.63	0.02	0.33	7.5	
PNLF	Grp	(m-M)	10	−1.69	0.03	0.20	2.2	less ComaI/II
SNII	Grp	(m-M)	5	−1.80	0.12	0.36	1.4	
SNII	Grp	(m-M)	4	−1.76	0.12	0.22	1.1	less N7331
TF	Grp	(m-M)	26	−1.69	0.03	0.41	2.1	
TF (MkII)	Grp	5logd	29	13.55	0.08	0.59	2.1	
Dn-sigma	Grp	5logd	28	13.64	0.05	0.44	1.9	
SNIa (M_{max})	Grp	5logd	6	13.92	0.08	0.38	3.6	
SNIa (Δm_{15})	Grp	5logd	6	14.01	0.08	0.40	3.6	
SNIa (M_{max})	gxy	5logd	5	13.86	0.12	0.54	4.9	
SNIa (Δm_{15})	gxy	5logd	5	14.01	0.12	0.43	3.2	
SNIa (M_{max})	gxy	5logd	4	13.64	0.13	0.22	1.0	less N5253
SNIa (Δm_{15})	gxy	5logd	4	13.87	0.13	0.30	1.8	less N5253
Theory				−1.81		0.11		

Note. — Columns: Name of the estimator, comparison by group or by galaxy, estimator's zero point based on Mpc ($m-M$) or Hubble flow (5logd km/s), number of comparison points, mean difference between SBF and the estimator, expected error in this mean based on error estimates, rms scatter in the comparison, χ^2/N, and comments.

Table 5. SBF Distances to Groups.

Group	Example	RA	Dec	v_{ave}	N	$(m-M)$	$\pm$	d	$\pm$
LocalGrp	N0224	10.0	41.0	−300	2	24.43	0.08	0.77	0.03
M81	N3031	147.9	69.3	−40	2	27.78	0.08	3.6	0.2
CenA	N5128	200.0	−39.0	550	3	28.03	0.10	4.0	0.2
N1023	N1023	37.0	35.0	650	4	29.91	0.09	9.6	0.4
LeoI	N3379	161.3	12.8	900	5	30.14	0.06	10.7	0.3
N7331	N7331	338.7	34.2	800	2	30.39	0.10	12.0	0.6
UMa	N3928	180.0	47.0	900	5	30.76	0.09	14.2	0.6
ComaI	N4278	184.4	29.6	1000	3	30.95	0.08	15.5	0.6
ComaII	N4494	187.2	26.1	1350	3	31.01	0.08	15.9	0.6
Virgo	N4486	187.1	12.7	1150	27	31.03	0.05	16.1	0.4
Dorado	N1549	63.7	−55.7	1300	6	31.04	0.06	16.1	0.5
Fornax	N1399	54.1	−35.6	1400	26	31.23	0.06	17.6	0.5

Note. — Columns: Group name, sample member, RA and Dec (B1950), mean heliocentric velocity, number of SBF distances, SBF distance modulus and error, and SBF distance (Mpc) and error.

REFERENCES

Aaronson, M., Huchra, J., Mould, J., Schechter, P., & Tully, R.B. 1982, ApJ, 258, 64.

Ajhar, E. A. & Tonry, J. L. 1994, ApJ, 429, 557.

Burstein, D., & Heiles, C. 1984, ApJS, 54, 33.

Buta, R. & Williams, K.L. 1995, AJ, 109, 543.

Buzzoni, A. 1993, A&A, 275, 433.

Buzzoni, A. 1995, ApJS, 98, 69.

Cardelli, J.A., Clayton, G.C., & Mathis, J.S. 1989, ApJ, 345, 245.

Ciardullo, R., Jacoby, G.H. & Tonry, J.L. 1993, ApJ, 419, 479.

Cohen, J.G., Frogel, J.A., Persson, S.E., & Elias, J.H. 1981, ApJ, 249, 481.

de Vaucouleurs, A., Longo, G. 1988, University of Texas monograph #5.

de Vaucouleurs, G., de Vaucouleurs, A., Corwin, H. G., Jr., Buta, R. J., Paturel, G., & Fouqué, P. 1991, Third Reference Catalog of Bright Galaxies (New York: Springer).

Eastman, R.G, Schmidt,B.P. & Kirshner, R.P. 1996, ApJ, Aug1, 000.

Faber, S. M., Wegner, G., Burstein, D., Davies, R. L., Dressler, A., Lynden-Bell, D., & Terlevich, R. J. 1989, ApJS, 69, 763.

Ferrarese, L. et al. 1996, ApJ, 000, 000.

Freedman, W. L. 1989, AJ, 98, 1285.

Freedman, W.L. & Madore, B.F. 1990, ApJ, 365, 186.

Freedman, W.L., et al. 1994, ApJ, 427, 628.

Graham, J.A., et al. 1996, in preparation.

Green, E. M., Demarque, P., & King, C. R. 1987, The Revised Yale Isochrones and Luminosity Functions, (Yale, New Haven).

Hamuy, M., Phillips, M.M., Maza, J., Suntzeff, N.B., Schommer, R.A., & Aviles, R. 1995, AJ, 109, 1.

Hughes S.M. 1996, private communication.

Jacoby, G.H., Branch, D., Ciardullo, R., Davies, R.L., Harris, W.E., Pierce, M.J., Pritchet, C.J., Tonry, J.L., Welch D.L. 1992, PASP, 104, 599.

Jacoby, G.H., Ciardullo, R., & Harris, W.E. 1996 ApJ462 1.

Jensen, J. B., Luppino, G. A., & Tonry, J. L. 1996, ApJ, in press.

Landolt, A.U. 1992, AJ, 104, 340.

Lorenz, H., Bohm, P., Capaccioli, M., Richter, G. M., & Longo, G. 1993, A&A, 277, L15.

Luppino, G.A. & Tonry, J.L. 1993, ApJ, 410, 81.

Lynden-Bell D. et al. 1988, ApJ, 326, 19.

Metzger, M.R., Tonry, J.L., & Luppino, G.A. 1993, ASP. Conf. Ser,. 52,, 300.

Pahre, M. A. & Mould, J. R. 1994, ApJ, 433, 567.

Phillips, M.M. 1993, ApJ, 413, L105.

Poulain, P. & Nieto, J-L. 1994, A&AS, 103, 573.

Press W.H., Teukolsky, S.A. Vetterling, W.T., & Flannery, B.P. 1992, Numerical Recipes, second edition; New York: Cambridge Univ. Press.

Riess, A.G., Press, W.H., & Kirshner, R.P. 1995, ApJ, 438, L17.

Ruiz-Lapuente, P. 1996, ApJ, 465, L83.

Saha, A., et al. 1995, ApJ, 438, 8.

Saha, A., Sandage, A., Labhardt, L., Tammann, G.A., Macchetto, F.D., & Panagia. N. 1996a, ApJ, 000, 000.

Saha, A., et al. 1996b, ApJ, in press.

Sandage, A. & Tammann G.A. 1993, ApJ, 415, 1.

Sandage, A., Saha, A., Tammann, G.A., Labhardt, L., Panagia. N., & Macchetto, F.D. 1996, ApJ, 000, 000.

Schechter, P.L., Mateo, M. & Saha, A. 1993, PASP, 105, 1342.

Schneider, D. 1996, private communication.

Silbermann, N.A. et al. 1996a, preprint.

Silbermann, N.A. et al. 1996b, poster presented at the STScI meeting on the Extragalactic Distance Scale, May 1996.

Simard, L. & Pritchet, C. J. 1994, ApJ, 107, 503.

Sodemann, M. & Thomsen, B. 1995, AJ, 110, 179.

Sodemann, M. & Thomsen, B. 1996, AJ, 111, 208.

Tammann, G.A. 1992, Phys. Scr, T43, 31.

Tanvir, N., et al. 1995, Nature, 377, 27.

Tiede, G.P., Frogel, J. A., & Terndrup, D. M. 1995, AJ, 110, 2788.

Tonry, J.L. 1991, ApJ, 373, L1.

Tonry, J.L., Ajhar, E.A., & Luppino, G.A. 1989, ApJ, 346, L57.

Tonry, J.L., Ajhar, E.A., & Luppino, G.A. 1990, AJ, 100, 1416.

Tonry, J.L., & Davis, M. 1981, ApJ, 246, 680.

Tonry, J.L., Luppino, G.A., & Schneider, D.P., 1988, in Proceedings of the ASP Meeting on The Extragalactic Distance Scale, S. van den Bergh & C. Pritchet, eds.

Tonry, J.L. & Schneider, D.P. 1988, AJ, 96, 807.

Tully, R. B. 1996, private communication.

Worthey, G. 1993, ApJ, 409, 530.

Worthey, G. 1993, ApJ, 418, 947.

Worthey, G. 1994, ApJS, 95, 107.

Worthey G. 1996, private communication.

Yi, S. 1996, private communication.

This preprint was prepared with the AAS LaTeX macros v4.0.

Fig. 1.— Histograms of photometric differences in surface photometry between all pairs of observations (including published photoelectric data) of the same galaxies, in V (upper panel), I (center panel), and $(V-I)$ (lower panel) The points and wider Gaussian curves are the distribution of pairwise differences prior to application of run offsets, and the histograms and narrower Gaussians reflect the improvement from using these offsets. This pair by pair comparison is used to define zero point offsets between runs and bring all the photometry onto the same scale as photoelectric photometry.

Fig. 2.— Differences for multiple observations of the same galaxy in $(V-I)_0$ (upper panel) and $\overline{m}_I$ (lower panel). Each histogram shows the distribution of the difference between multiple observations divided by the estimated error. A Gaussian of unity variance and normalization equal to the number of pairs is shown for comparison.

Fig. 3.— The distribution of $\overline{m}_I$ as a function of $(V-I)_0$ for six groups: NGC 1023, Leo, UMa, Coma I&II (including both the NGC 4278 and NGC 4494 subgroups), Virgo, and Fornax. Spiral galaxies (i.e. RC3 T-type $T > 0$) are indicated with filled symbols, and the vertical error bar shows our estimate of rms group depth (derived from the angular extent of the group across the sky) multiplied by 5 as an expectation for the peak-to-peak depth of the cluster. Only in Fornax and in Leo are the SBF measurement errors as big as the putative depth of the group. The three small squares in the Virgo panel are for NGC 4600, NGC 4365, and NGC 4660, galaxies which we believe to be foreground or background even though they meet the Virgo group criteria. The lines show the SBF relation for each of these groups from our overall fit to all the data.

Fig. 4.— The distribution of $\overline{m}_I$ - $\langle \overline{m}_I^0 \rangle$ as a function of $(V-I)_0$ for all galaxies belonging to our groups. A line through $(1.15, 0.0)$ with the mean slope of the SBF-color relation is drawn. The four spiral galaxies for which we have both Cepheid and SBF distances, NGC 224, NGC 3031, NGC 3368, and NGC 7331, are plotted as large, solid hexagons and demonstrate that SBF is the same for spiral bulges as for elliptical and S0 galaxies. The round, solid points above the line are various locations in NGC 205, and the round, solid points below the line are NGC 147 and NGC 185 (not used in the fit). The inset shows NGC 205 again, along with NGC 5253 and IC 4182, which are placed according to their Cepheid distances.

Fig. 5.— The $(V-I)_0$ corrected $\overline{m}_I$ quantity, $\overline{m}_I^0$, as a function of Mg_2 and B_T magnitude (from the RC3) in the Virgo and Fornax clusters. The lack of correlation indicates that $\overline{m}_I$ is a one-parameter function of stellar population, and $(V-I)_0$ adequately delineates the variations of stellar population over this color range.

Fig. 6.— The mean $\langle \overline{m}_I^0 \rangle$ derived for our groups compared to other distance estimators: Cepheids, SNII, SNIa (treated as standard candles), and SNIa (correcting the peak magnitude for the rate of decline Δm_{15}. The other estimators' distances are either in terms of Mpc, expressed as a distance modulus $(m-M)$, or in terms of km/s, plotted as 5 times the logarithm. The lines are drawn according to a weighted fit of unity slope between each set of distances. The "fast decline" SNIa

are plotted as solid points, but are not used in any of the fits. NGC 7331 is drawn as a solid point in the SNII comparison because the SNII distance is discordant with both SBF and Cepheids. Above each distance comparison is a histogram of the differences $\langle \overline{m}_I^0 \rangle - (m-M)$ or $\langle \overline{m}_I^0 \rangle - 5 \log d$.

Fig. 7.— Same as Figure 6, but comparing SBF and the tertiary estimators PNLF, TF (Mpc zero point), TF (from MarkII catalog), and $D_n-\sigma$. The recent PNLF distances for the ComaI&II galaxies are plotted as solid symbols.

Fig. 8.— Comparison of the theoretical model predictions of $\overline{M}_I$ from Worthey with our empirical calibration from Cepheids, $\overline{M}_I = -1.74 + 4.5[(V-I)_0 - 1.15]$, drawn as a dashed line. The solid line shows a fit to the theoretical models using the empirical slope: the two differ by 0.07 mag in zero point or 0.015 mag in color. The models have ages of 5, 8, 12, and 17 Gyr (older are redder and fainter), and their metallicity relative to solar is indicated by point type.

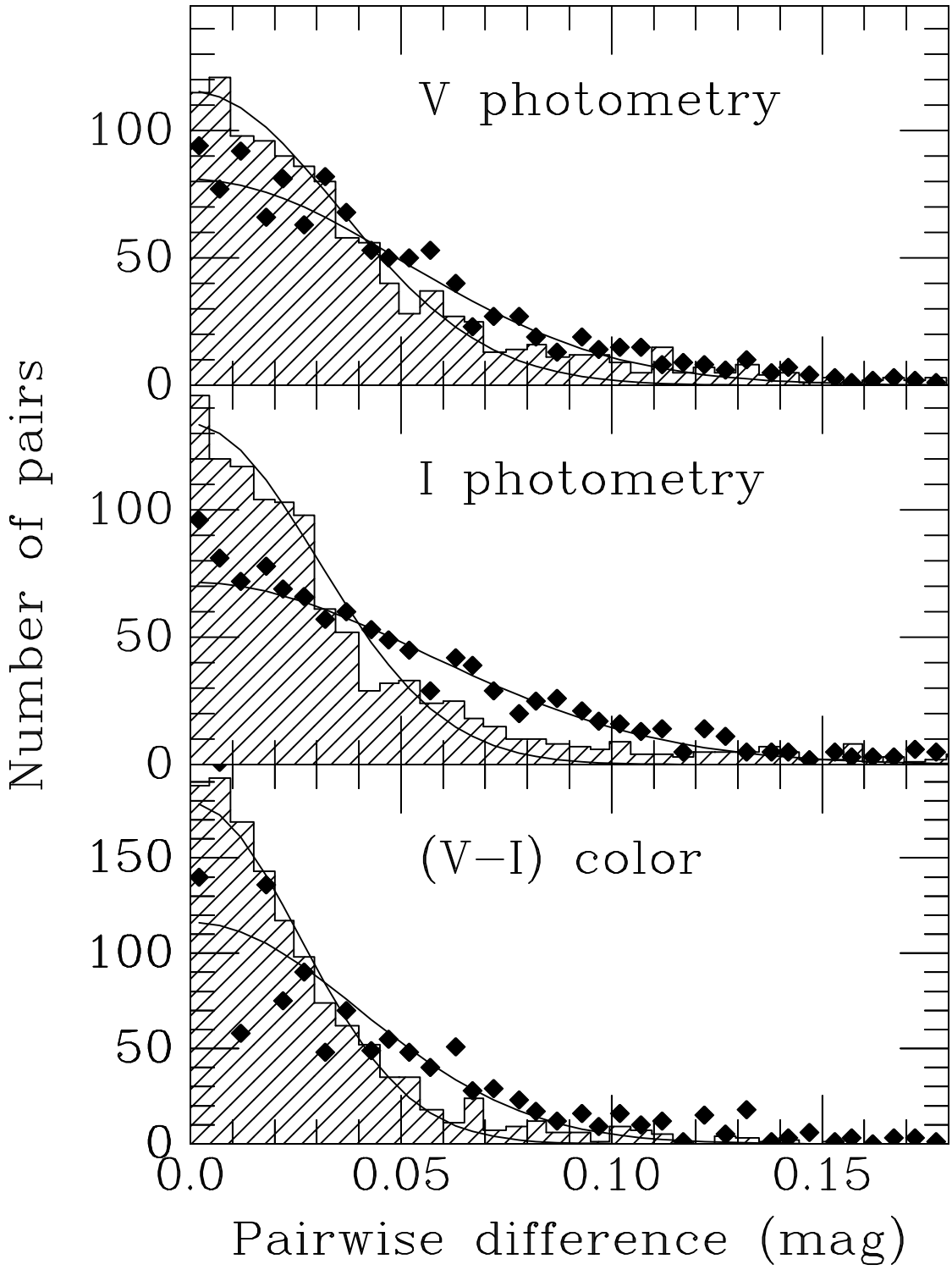
V photometry
I photometry
(V−I) color
Number of pairs
Pairwise difference (mag)
0
50
100
150
0.0
0.05
0.10
0.15

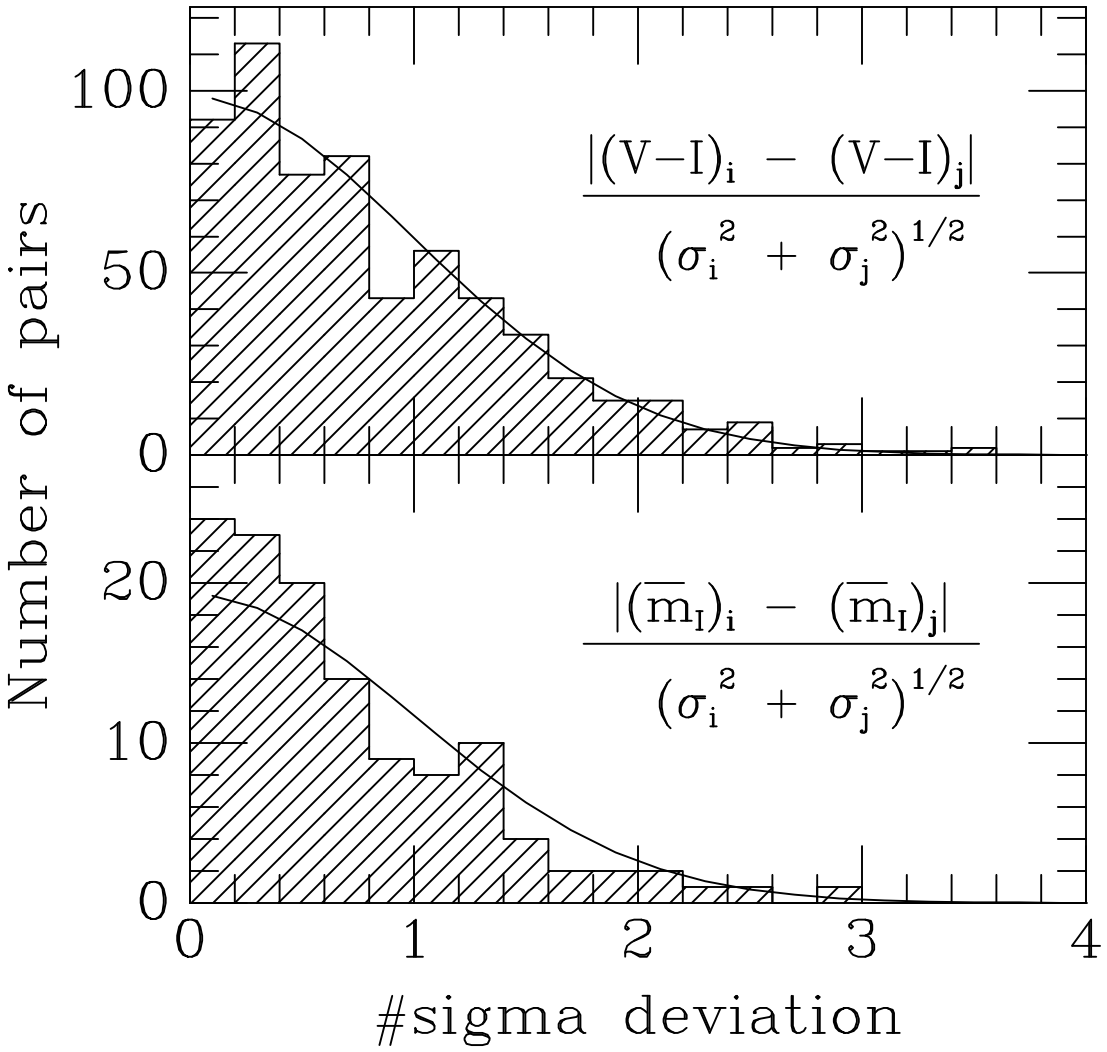
100
50
0
20
10
0
0
1
2
3
4
Number of pairs
#sigma deviation
$\frac{|(V-I)_i - (V-I)_j|}{(\sigma_i^2 + \sigma_j^2)^{1/2}}$
$\frac{|(\overline{m}_I)_i - (\overline{m}_I)_j|}{(\sigma_i^2 + \sigma_j^2)^{1/2}}$

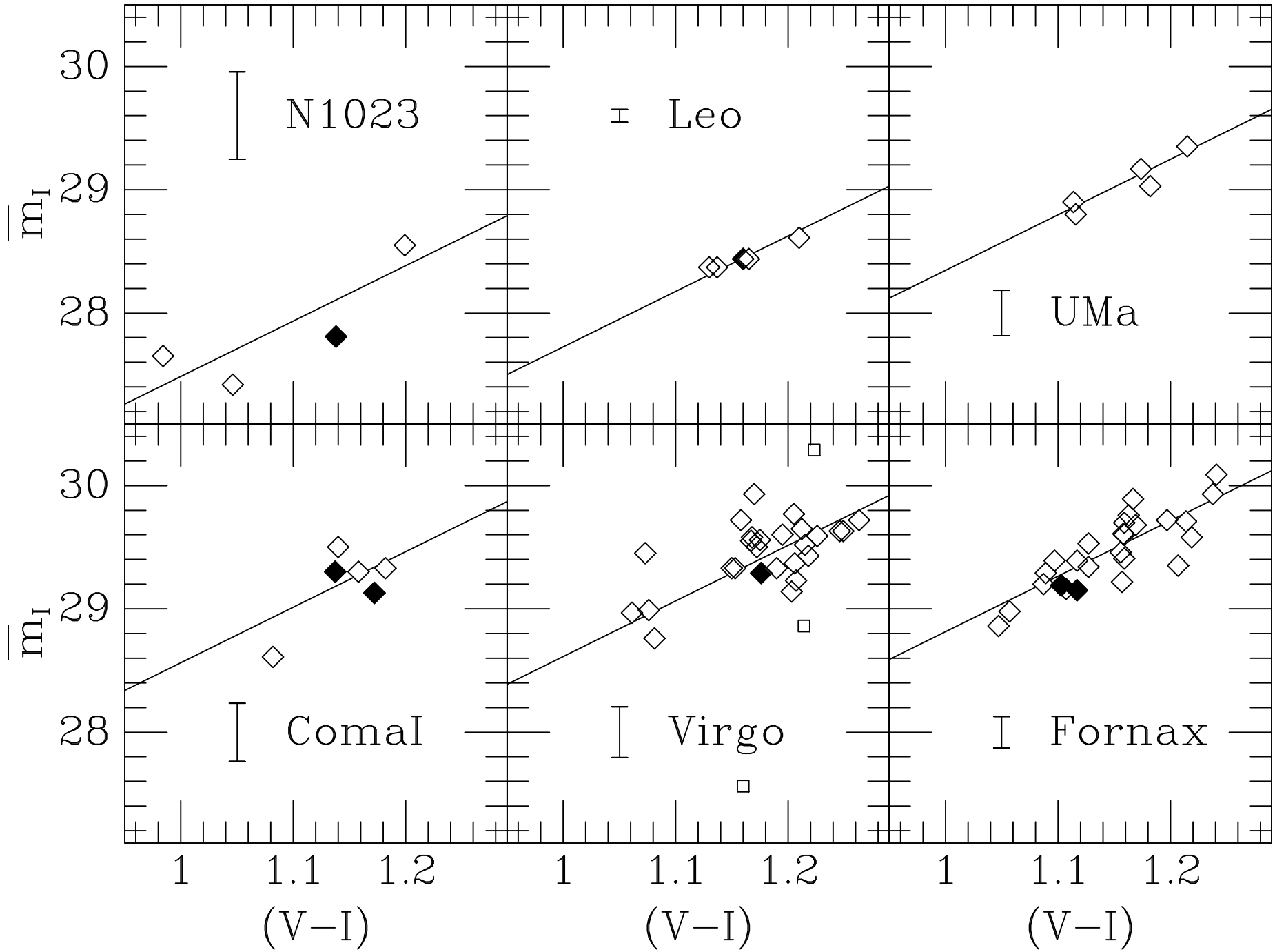
N1023
Leo
UMa
ComaI
Virgo
Fornax
$\overline{m}_I$
$\overline{m}_I$
30
29
28
30
29
28
1
1.1
1.2
1
1.1
1.2
1
1.1
1.2
(V−I)
(V−I)
(V−I)

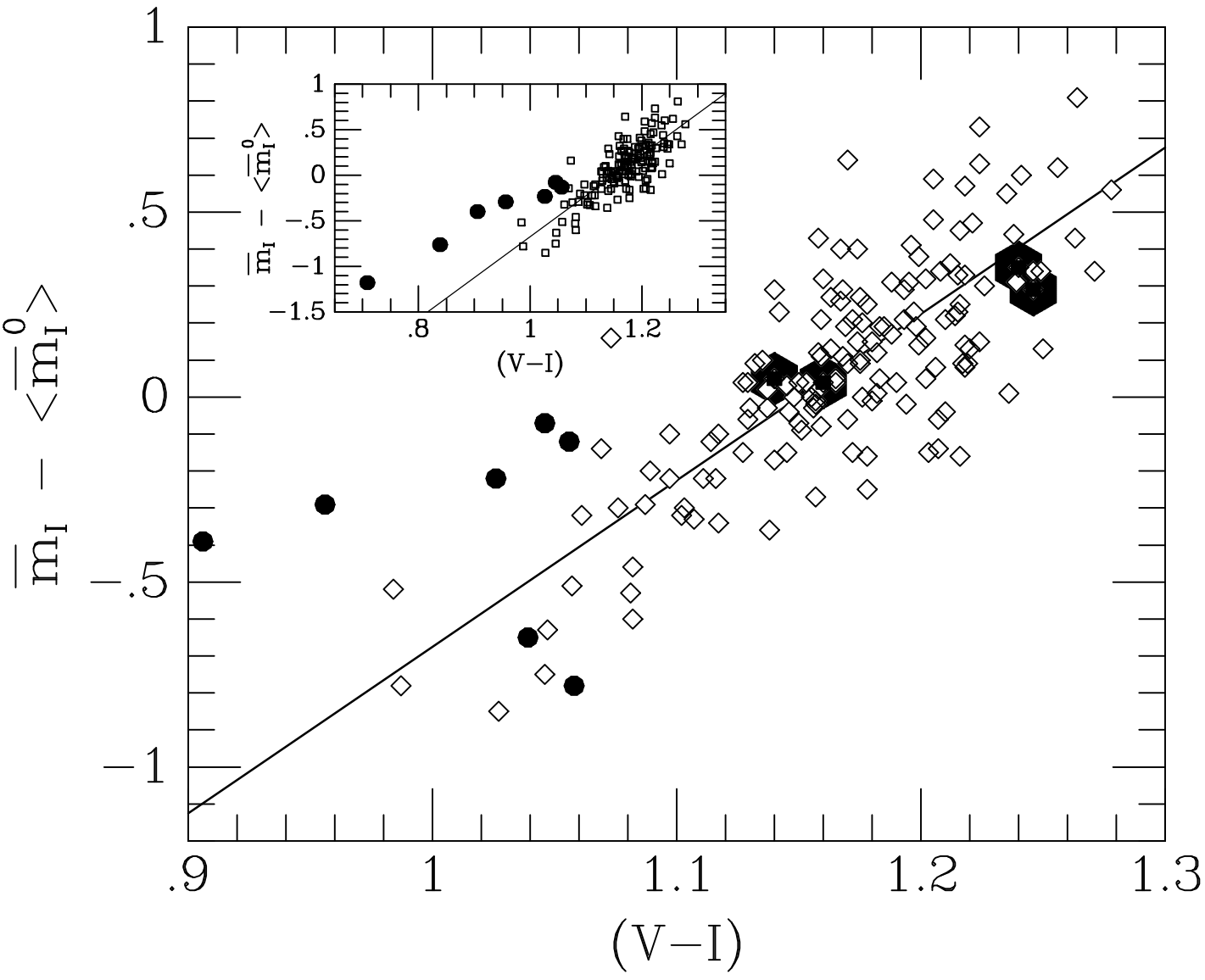
1
.5
0
−.5
−1
.9
1
1.1
1.2
1.3
(V−I)
$\overline{m}_I - \langle \overline{m}_I^0 \rangle$
1
.5
0
−.5
−1
−1.5
.8
1
1.2
(V−I)
$\overline{m}_I - \langle \overline{m}_I^0 \rangle$

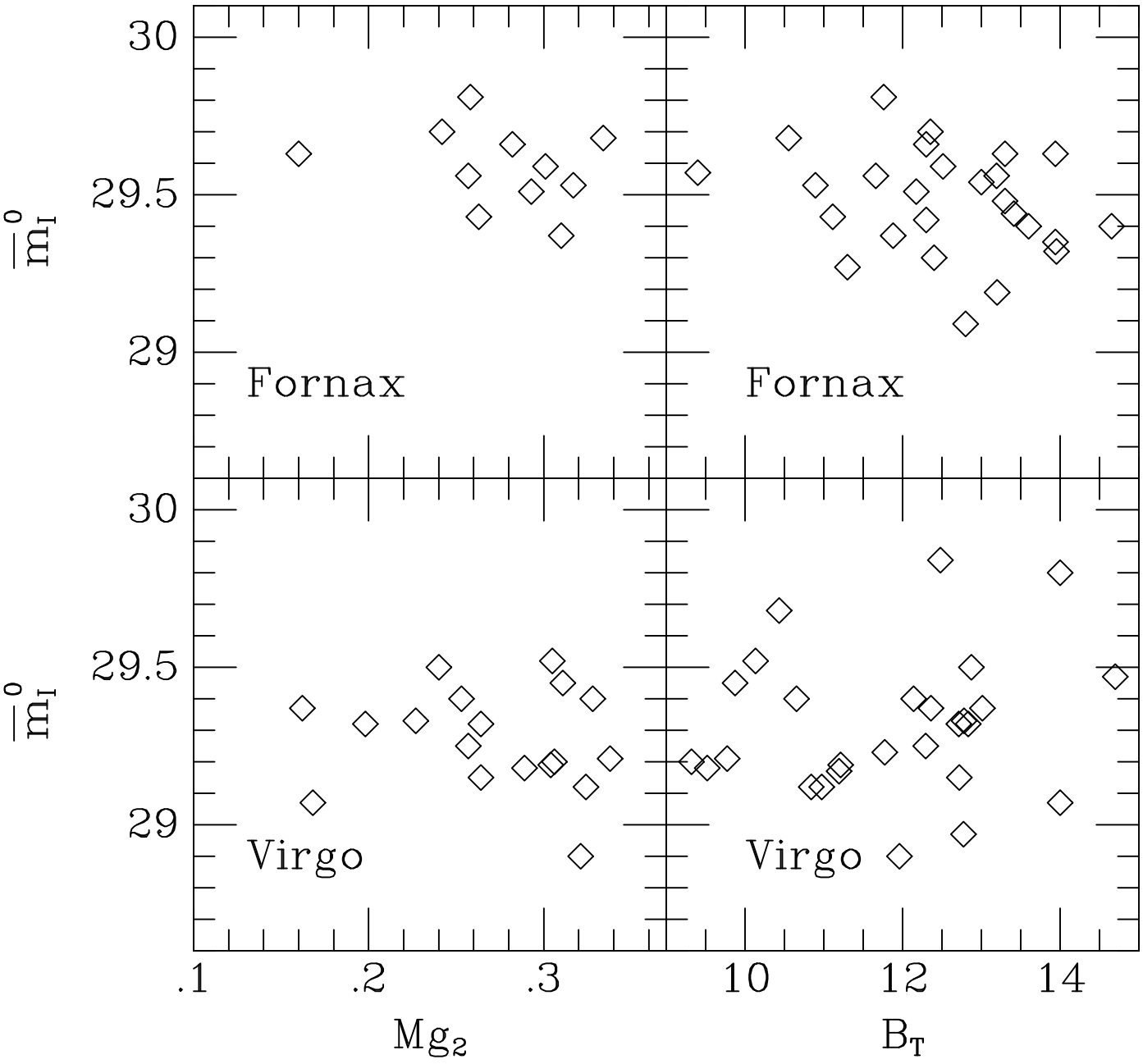
30
29.5
29
30
29.5
29
$\overline{m}_I^0$
$\overline{m}_I^0$
Fornax
Fornax
Virgo
Virgo
.1
.2
.3
10
12
14
Mg_2
B_T

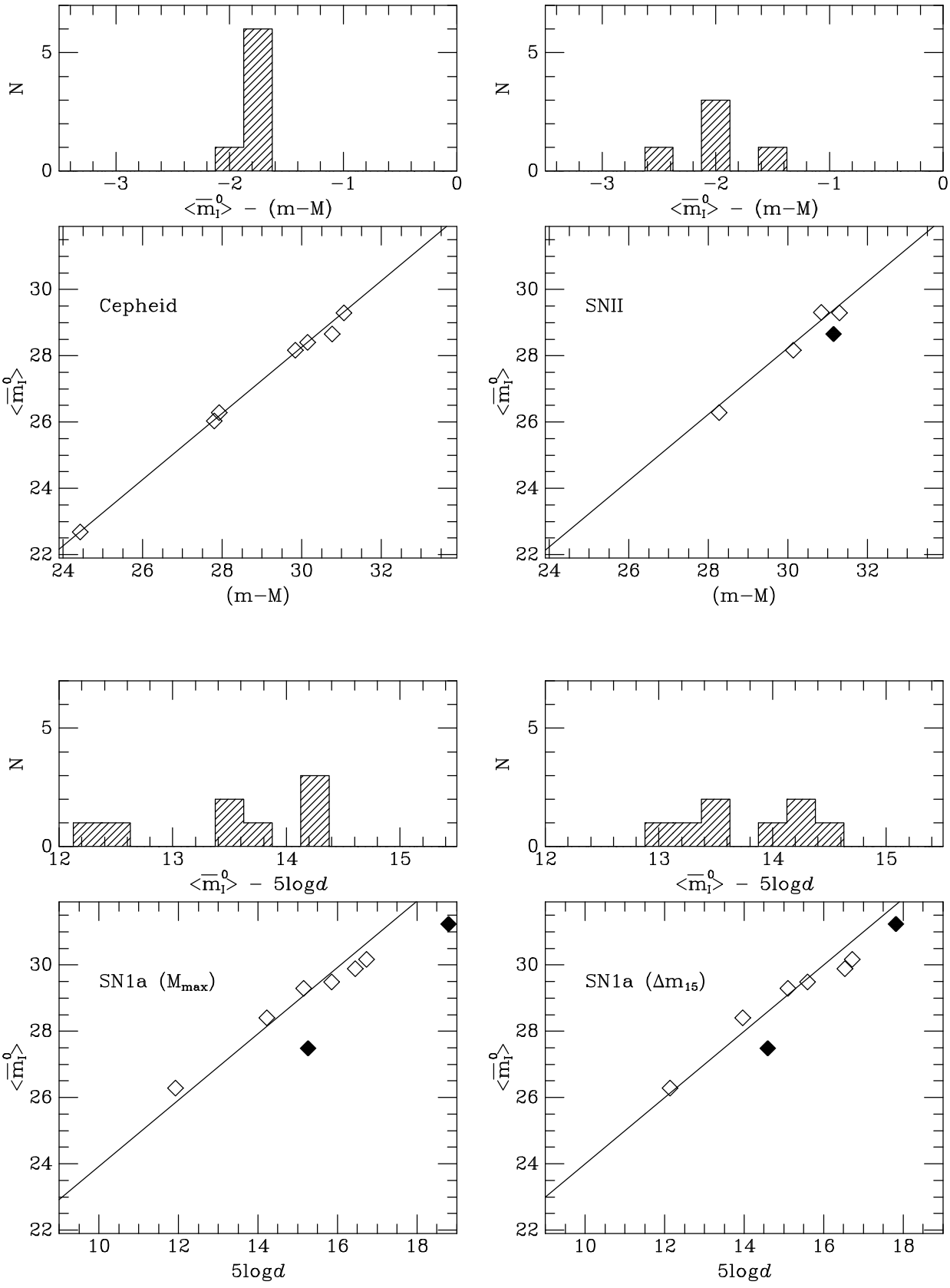
N
$\langle \overline{m}_I^0 \rangle$ − (m−M)
Cepheid
SNII
$\langle \overline{m}_I^0 \rangle$
(m−M)
$\langle \overline{m}_I^0 \rangle$ − 5log$d$
SN1a (M_{max})
SN1a (Δm_{15})
5log$d$

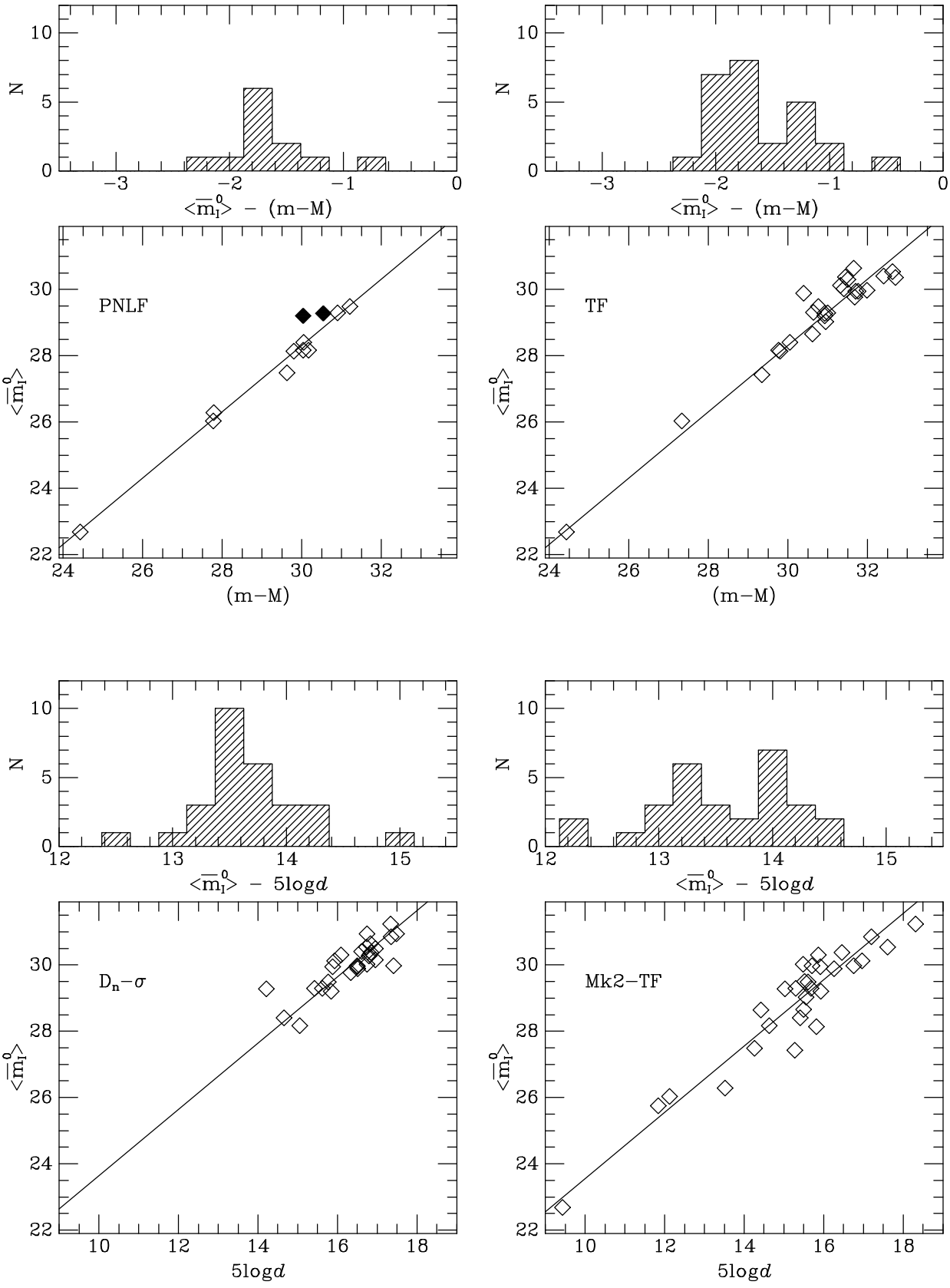
N
$\langle \overline{m}_I^0 \rangle$ − (m−M)
PNLF
TF
$\langle \overline{m}_I^0 \rangle$
(m−M)
$\langle \overline{m}_I^0 \rangle$ − 5log$d$
$D_n-\sigma$
Mk2−TF
5log$d$

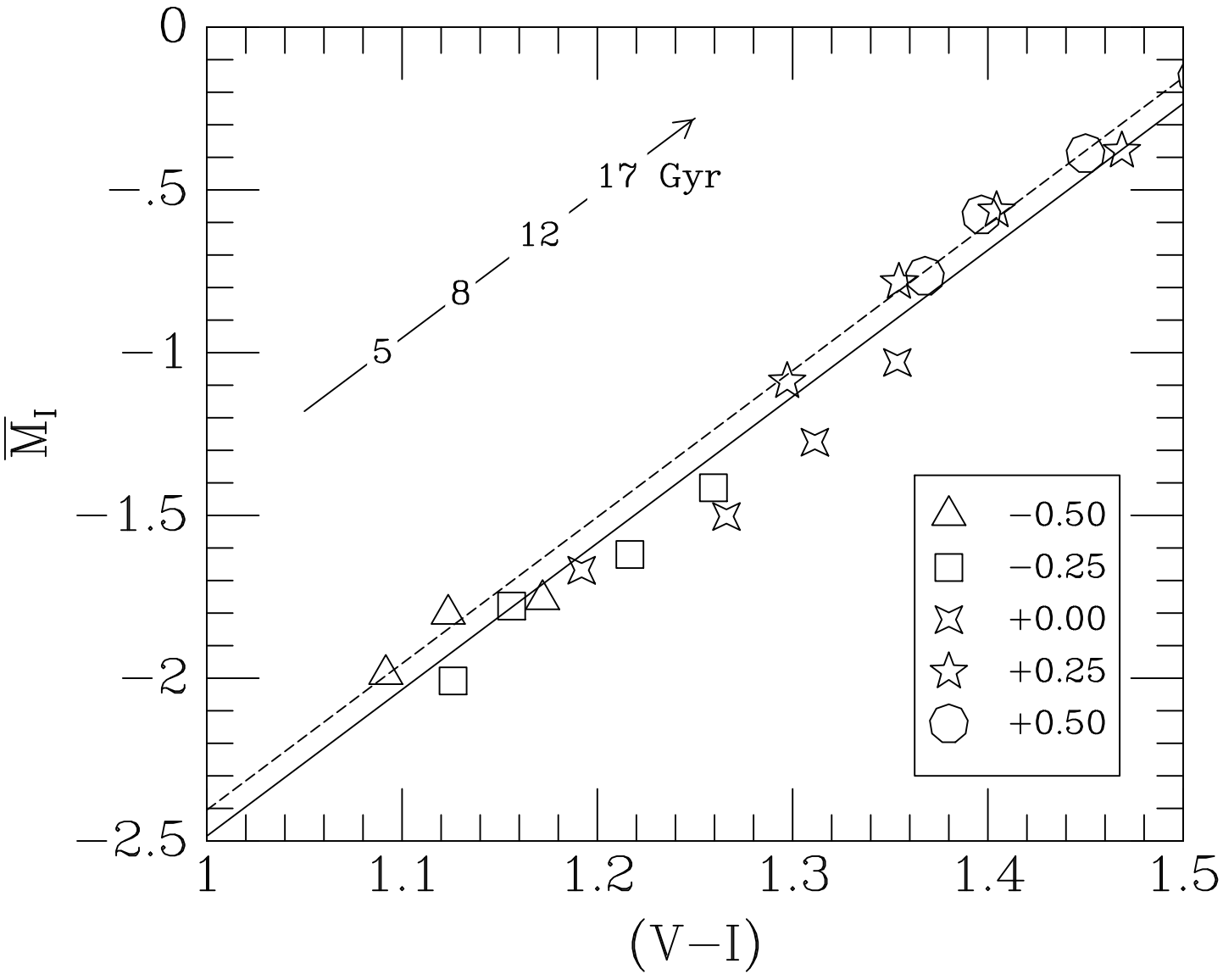
0
−.5
−1
−1.5
−2
−2.5
1
1.1
1.2
1.3
1.4
1.5
$\overline{M}_I$
(V−I)
17 Gyr
12
8
5
−0.50
−0.25
+0.00
+0.25
+0.50